Original

Vascular response after implantation of biolimus A9-eluting stent with bioabsorbable polymer and everolimus-eluting stents with durable polymer. Results of the optical coherence tomography analysis of the BIOACTIVE randomized trial

Daniel Chamié[a,*], Breno O. Almeida[b], Fábio Grandi[c], Evandro M. Filho[a], J. Ribamar Costa Jr.[a], Ricardo Costa[a], Rodolfo Staico[a], Dimytri Siqueira[a], Fausto Feres[a], Luiz Fernando Tanajura[a], Marinella Centemero[a], Áurea J. Chaves[a], Andrea Abizaid[a], Amanda G.M.R. Sousa[a], Alexandre Abizaid[a]

[a] *Instituto Dante Pazzanese de Cardiologia, São Paulo, SP, Brazil*
[b] *Hospital Santa Marcelina, São Paulo, SP, Brazil*
[c] *Cardiovascular Research Center, São Paulo, SP, Brazil*

ARTICLE INFO

Article history:
Received 1 December 2014
Accepted 8 February 2015

Keywords:
Drug-eluting stents
Tomography, optical coherence
Percutaneous coronary intervention

ABSTRACT

Background: In BIOACTIVE study, we evaluated vascular responses after the implant of biolimus A9-eluting stent (BES; BioMatrix™) and the everolimus-eluting stent (EES; XIENCE V™). In this study, we present the optical coherence tomography analysis (OCT) 6 months post-intervention.
Methods: Patients were randomized to treatment with BES (n = 22) or EES (n = 18). The primary outcome was the frequency of non-covered, poorly positioned struts by OCT.
Results: OCT was performed in 26 patients (BES: n = 15; EES: n = 11) and 749 tomographic images and 7,725 stent struts were analyzed. BES and EES showed similar luminal and stent areas. Neointimal hyperplasia area, neointimal thickness and the percentage of in-stent obstruction (8.44 ± 5.10% vs. 9.21 ± 6.36%; p = 0.74) were similar. The rates of not covered struts (BES: 2.10 ± 3.60% vs. ESS: 2.46 ± 2.15%, p = 0.77) and poorly positioned struts (BES: 0.48 ± 1.48% vs. EES 0.44 ± 1.05%, p = 0.94) were similarly low. The frequency of frames with signs consistent with peri-strut inflammatory infiltrate was low and similar between BES (15.53 ± 20.77%) and EES (11.70 ± 27.51%; p = 0.68).
Conclusions: The second-generation drug-eluting stents BES and EES were equally effective at suppressing the neointimal formation after 6 months, with favorable vascular responses. The frequency of frames with peri-strut infiltrate signals per patient was low, and lower than that observed historically with first-generation drug-eluting stents.

Resposta vascular após implante de stents liberadores de biolimus A9 com polímero bioabsorvível e stents liberadores de everolimus com polímero durável. Resultados da análise de tomografia de coerência óptica do estudo randomizado BIOACTIVE

Palavras-chave:
Stents farmacológicos
Tomografia de coerência óptica
Intervenção coronária percutânea

RESUMO

Introdução: No estudo BIOACTIVE, avaliamos as respostas vasculares após implante do stent eluidor de biolimus A9 (SEB; BioMatrix™) e o stent eluidor de everolimus (SEE; XIENCE V™). Apresentamos a análise de tomografia de coerência óptica (OCT) 6 meses pós-intervenção.
Métodos: Os pacientes foram randomizados para tratamento com SEB (n = 22) ou SEE (n = 18). O desfecho primário foi a frequência de hastes não cobertas e mal apostas pela OCT.
Resultados: A OCT foi realizada em 26 pacientes (SEB: n = 15; SEE: n = 11) e foram analisadas 749 imagens tomográficas e 7.725 hastes de stent. SEB e SEE apresentaram áreas luminais e dos stents semelhantes. A área de hiperplasia neointimal, a espessura neointimal e o porcentual de obstrução intra-stent (8,44

DOI of original article: http://dx.doi.org/10.1016/j.rbci.205.02.001
* Corresponding author: Avenida Dr. Dante Pazzanese, 500, Ibirapuera, CEP: 04012-180, São Paulo, SP, Brazil.
E-mail: daniel.chamie@gmail.com (D. Chamié).
Peer Review under the responsability of Sociedade Brasileira de Hemodinâmica e Cardiologia Intervencionista.

± 5,10% vs. 9,21 ± 6,36%; p = 0,74) foram similares. As taxas de hastes não cobertas (SEB: 2,10 ± 3,60% vs. SEE: 2,46 ± 2,15%; p = 0,77) e mal apostas (SEB: 0,48 ± 1,48% vs. SEE 0,44 ± 1,05%; p = 0,94) foram baixas e semelhantes. A frequência de *frames* com sinais compatíveis com infiltrado inflamatório peri-haste foi baixa e similar entre SEB (15,53 ± 20,77%) e SEE (11,70 ± 27,51%; p = 0,68).
Conclusões: Stents farmacológicos de segunda geração SEB e SEE se mostraram igualmente eficientes em suprimir a formação neointimal aos 6 meses, com respostas vasculares favoráveis. A frequência de *frames* com sinais de infiltrado peri-haste por paciente foi baixa, e menor do que a historicamente observada com os stents farmacológicos de primeira geração.

Introduction

Drug-eluting stents (DES), designed under the concept of locally applying an antiproliferative agent on the vascular wall in a controlled manner, have met their primary endpoint of reducing excessive neointimal formation, commonly observed after coronary angioplasty with balloon and bare-metal stent (BMS) implantation.[1,2] High antiproliferative efficacy has resulted in a significant reduction in restenosis rates and need for new coronary revascularization in a wide variety of clinical and anatomical scenarios,[3-8] making DES implantation the standard treatment strategy during percutaneous coronary intervention (PCI) procedures in many regions of the world.

However, the widespread use of DES and longer follow-up of patients treated with this technology disclosed a significantly higher incidence of late- and very-late thrombosis than in those seen after BMS implantation.[9-11]

Although late/very late stent thrombosis is a multifactorial phenomenon, incomplete strut coverage due to delay in cellular matrix and functioning endothelium formation, chronic inflammatory reactions in the vessel wall, vascular remodeling, and acquired late malapposition were demonstrated after the implantation of first-generation DES.[12-16] In general, these DES consisted of stainless steel platforms with relatively thick metal struts that eluted high doses of sirolimus or paclitaxel *via* durable polymeric carriers distributed around the entire metal surface. In particular, the durable polymers of the first-generation DES – in permanent contact with the vessel wall – were associated with local hypersensitivity reactions.[12]

These findings led to the development of new DES, aiming to reduce toxicity to the vascular wall and increase the biocompatibility of these devices, although without losing the antiproliferative efficacy displayed by the first-generation DES. In this sense, a number of modifications were implemented: platforms made of new metallic alloys; thinner struts; improved delivery systems; new antiproliferative drugs; use of lower doses of drugs; new polymeric matrices that are thinner, more biocompatible, and even bioresorbable; polymer applied directly to the abluminal side of the stent struts; and drug carrying and elution by non-polymeric platforms, etc.[17]

The BIOACTIVE study aimed to assess vascular responses after implantation of two second generation DES – BioMatrix™ (biolimus A9-eluting stent, utilizing a biodegradable polymer), and XIENCE V™ (everolimus-eluting stent, utilizing a durable, biocompatible fluoropolymer), which incorporated one or more of the aforementioned characteristics. For that purpose, optical coherence tomography (OCT) images were used, which, through high-resolution CT images, allow accurate assessment of the vascular repair process after coronary stenting.[18,19] This study aimed to present the OCT analysis at 6 months post-intervention.

Methods

Study design and population

BIOACTIVE is a prospective, randomized trial of the investigators' initiative, in two centers (Instituto Dante Pazzanese de Cardiologia and Hospital Santa Marcelina), located in São Paulo, SP, Brazil, which aimed to assess the coronary vascular response six months after the implantation of the second-generation XIENCE V™ and BioMatrix™ DES. The primary endpoint of the study consisted of the combined assessment of two outcomes after six months: 1– evaluation of coronary endothelial function – quantified by quantitative coronary angiography (QCA) through changes in the peri-stent luminal diameter (5 mm proximal and distal to the stent borders) between periods of rest, during sequential stimulation with cardiac pacemaker, and after administration of intracoronary nitroglycerin; and 2– quantification of the percentage coverage of the stent struts through OCT. Secondary endpoints consisted of the assessment of efficacy through QCA, intravascular ultrasound (IVUS), and OCT in the invasive 6 month follow-up.

Patients with *de novo* coronary lesions, with a maximum length of 20 mm and located in native coronary arteries with a diameter of 3.0 mm to 3.5 mm, were included in the study. Diabetic patients were excluded, as well as patients treated within 72 hours of an acute myocardial infarction (AMI) with ST-segment elevation. Patients with renal failure (serum creatinine > 2.0 mg/dL or estimated creatinine clearance < 30 mL/min) or severe left ventricular dysfunction (left ventricular ejection fraction < 30%) were also excluded. The main angiographic exclusion criteria were ostial lesions, bifurcation lesions, lesions in the left main coronary artery, or with the presence of thrombi or significant calcification.

The BIOACTIVE study was approved by the Research Ethics Committee of the participating institutions, and all patients signed an informed consent before randomization.

Characteristics of assessed stents

The BioMatrix™ stent has a stainless steel platform, 120 µm thick struts, coated with a 10 µm thick durable primer (parylene C) and an 11 µm thick polylactic acid (PLA) polymer, distributed only on the abluminal surface of the struts. This polymer carries the antiproliferative drug biolimus A9 and is designed to perform an initial fast release of approximately 40% of the drug. Subsequently, it is co-released with the remaining drug over a period of 6 to 9 months. Finally, the polymer is degraded into carbon dioxide and water.

The XIENCE V™ stent consists of a cobalt-chromium platform with thin struts (81 µm), coated with a durable and highly biocom-

patible fluoropolymer, distributed around the entire surface of the struts. This polymer carries the antiproliferative drug everolimus at a dose of 100 µm/mm² and is designed to release 80% of the total drug dose in the first 30 days after implantation.

Procedures

PCI procedures were performed according to the routines of the institutions and in accordance with current recommendations.[20,21] Pre-treatment with acetylsalicylic acid loading dose (300 mg) and clopidogrel (300 or 600 mg) was administered at least 24 hours before PCI to patients who were not chronic users of these medications. At the start of the procedure, anticoagulation with unfractionated heparin (100 IU/kg) was carried out with administration of additional bolus, where necessary, to maintain an activated clotting time ≥ 250 seconds.

After adequate positioning of the 0.014'' guidewire in the distal portion of the target vessel, patients were randomized in a 1:1 proportion to receive the BioMatrix™ or XIENCE V™ stents. Predilation of target lesions was not mandatory and the direct stenting was allowed. The indication for stent post-dilation was made at the operating physician's discretion and, when performed, was done with balloons, preferably noncompliant, with a shorter length than the nominal length of the implanted stent, in order to prevent inflations out of the treated segment.

Follow-up and endpoints

All patients were assessed by clinical consultation at the medical office or by telephone calls at 1; 6 and 12 months after the index PCI. Angiographic restudy, with IVUS and OCT, was performed after 6 months.

The present analysis shows the comparison of vascular response assessment by OCT, for which the primary endpoint was the difference in the percentage of struts not covered by neointimal tissue in both treatment groups. The secondary outcomes of the OCT analysis were as follows: frequency of strut malapposition, neointimal tissue area, percentage of stent obstruction by neointimal tissue, and neointimal thickness. The occurrence of major adverse cardiac events (death, nonfatal myocardial revascularization, and target-vessel revascularization) at 12 months was also computed as a secondary outcome.

All adverse events were adjudicated and classified by an independent adjudication committee blinded to the type of stent received by patients.

Acquisition and analysis of optical coherence tomography images

The OCT images were acquired with the commercially available time-domain OCT system (M3 System; LightLab Imaging, Westford, USA) or frequency-domain optical coherence tomography system (C7 XR; St. Jude Medical, St. Paul, USA). The techniques used for image acquisition with both OCT systems have been previously described in detail.[22,23] All images were stored in digital media and sent for analysis to an independent central laboratory (Cardiovascular Research Center, São Paulo, SP, Brazil). Analyses were performed using a dedicated and previously validated program[24] (QIvus™, version 3.0; Medis Medical Imaging, Leiden, Netherlands) and the operating physicians were blinded to the type of stent received by each patient.

After adjusting for the different pullback velocities of the imaging catheter provided by the two types of OCT equipment used, the analyses of tomographic vessel images were made at 0.6 mm intervals in the longitudinal direction, along the entire treated segment.

Automatic segmentation of the luminal contour (border between the lumen and the vessel intimal layer) was performed by the analysis program inside the predetermined segment, with manual adjustments made if necessary. Metal stent struts appear on the OCT as small points, or rounded or tapered structures that promote high reflection of the light signal emitted by the OCT catheter (blooming) and dorsal shadowing. Thus, a strut was considered for analysis only when the blooming + dorsal shadowing binomial was present. An automatic strut detection algorithm was used; false-positive or false-negative corrections were performed manually. The number of struts analyzed in each cross-sectional image along the segment of interest was then automatically computed. The contour traced along the inner surface of each strut was performed automatically and defined the stent area in each analyzed frame. Finally, the distance between the central points of the luminal face of each strut to the luminal contour was determined automatically by lines directed towards the center of gravity of the vessel (Fig. 1). When this distance was positive, the struts were classified as covered. Positive values of the distance between the stent strut and the lumen contour determined neointimal thickness in each individual strut. In case of negative distances, the struts were classified as uncovered (Fig. 2). If the negative distance was greater than the sum of the thickness of the strut + the thickness of the polymer (when present) + a correction factor for the minimum axial resolution of the OCT, the strut was classified as malapposed. Therefore, the cut-off points used to define strut malapposition varied according to the characteristics of each stent (BioMatrix™ = 150 µm and XIENCE V™ = 110 µm) (Fig. 3).

The neointimal area was determined based on the measurement of the neointimal thickness, located between the stent and luminal contour. Regions around the vessel circumference, with a negative distance between the stent and the lumen contours (no tissue coverage), were included for neointimal quantification (Fig. 3). After the

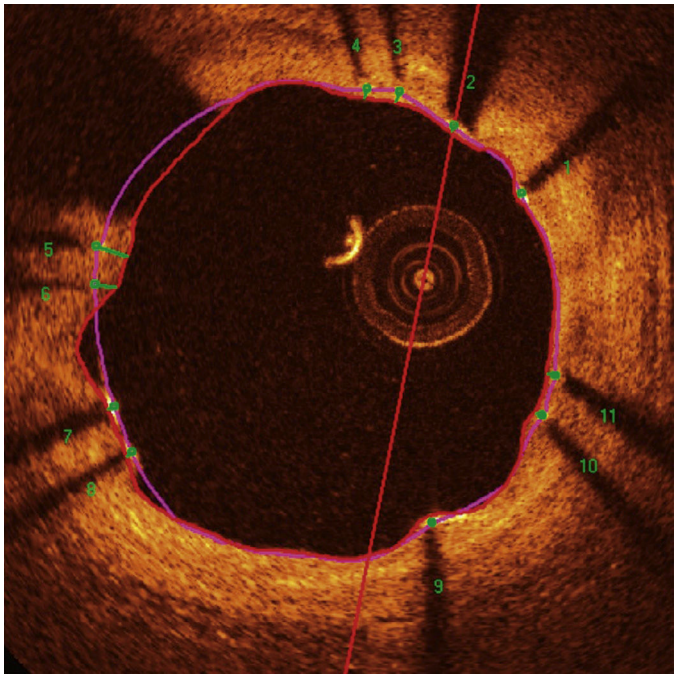

Figure 1. Optical coherence tomography analysis. The luminal contour is segmented automatically, following the border between the lumen and the intimal layer (red line). Then the stent struts – highly light-reflective structures, with dorsal shade – are identified by an automated algorithm. The points located on the luminal surface are connected to determine the stent area (pink line). The distances between the luminal surface of each strut to the luminal contour are automatically determined by a trajectory directed towards the center of the vessel (green lines).

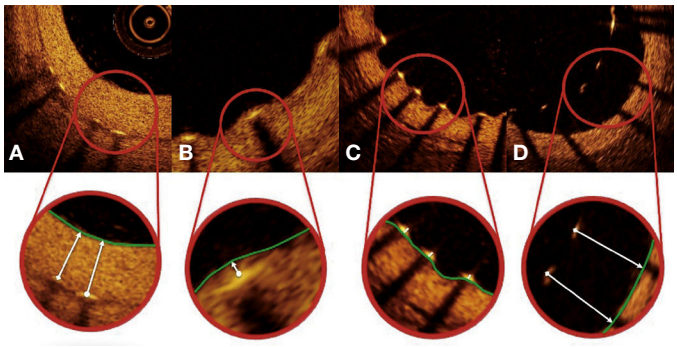

Figure 2. Strut coverage pattern. Each stent strut – present in each frame analyzed at 0.6 mm intervals from the treated segment – was evaluated. When the distance between the central point of the strut on its luminal surface in relation to the contour of the vascular lumen was positive, the strut was classified as covered, and the tissue thickness was determined by the distance in micrometers (panels **A** and **B**). When the distance was negative, the struts were classified as non-covered (panels **C** and **D**). If this negative distance was greater than the sum of the strut thickness + polymer thickness + drug, this strut was further classified as malapposed (panel **D**).

neointimal area was determined, stent obstruction percentage was computed for each analyzed frame by dividing the neointimal area by the stent area. The homogeneity of the circumferential and longitudinal distribution of neointimal hyperplasia along the treated segment was evaluated by visual assessment of scatter plots created for each case.

Finally, a qualitative assessment of neointimal tissue formed over the stent struts was performed. Peri-strut infiltrate regions were defined as homogeneous areas reflecting the optical signal with less intensity than the adjacent tissue, but without causing light attenuation.[25] Neoatherosclerosis was defined as the presence of lipid infiltrate or neointimal calcification.[26] Figure 4 illustrates examples of qualitative assessment of neointimal tissue formed over the stent struts.

Statistical analysis

Statistical analyses were performed using SPSS, version 20.0 (IBM Corp., Armonk, USA), and R software, version 3.1.1 (The R Foundation for Statistical Computing, Vienna, Austria).

Continuous variables are shown as mean and standard deviation and categorical variables as frequency and percentage. Categorical variables were analyzed by chi-squared test or Fisher's exact test, and continuous variables by Student's *t*-test and Mann-Whitney U-test, depending on variable distribution.

A generalized estimating equations model with first-order autoregressive covariance structure was used to adjust the analyses according to the pooled nature of the data from each patient (for instance, a patient with a stent placed in one vessel has dozens of frames and hundreds of struts analyzed). Thus, for a patient who received a long stent with more frames and struts analyzed, a different weight was computed as compared to another patient who received a short stent with fewer frames and struts analyzed.

All analyses were two-tailed and $p < 0.05$ was considered statistically significant.

Results

Characteristics of the population and procedures

Between July 2011 and April 2012, a total of 40 patients were included in the BIOACTIVE trial and randomized to receive the Bio-

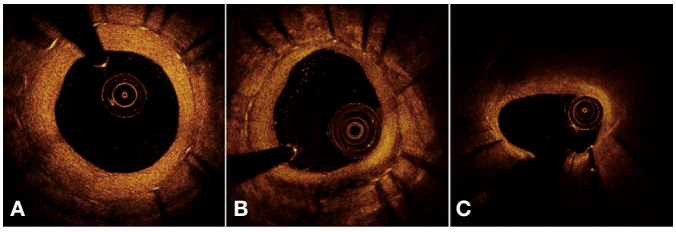

Figure 4. Qualitative assessment of neointimal tissue. In **A**, the cross-sectional image illustrates a pattern of normal vascular healing, characterized by high-intensity and homogeneous neointimal optical appearance. In **B**, an example of peri-strut infiltrate between 4 and 7 o'clock, characterized as a well-defined and homogeneous region that promotes low reflection of the optical signal, with less intensity than that of the surrounding tissue, but without causing lumen attenuation (allows for viewing of posterior structures). In **C**, an example of neoatherosclerosis, represented by lipid infiltration of neointimal tissue between 10 and 2 o'clock. Note significant attenuation of the optical signal, which prevents the visualization of the posterior structures in the region, including the stent struts.

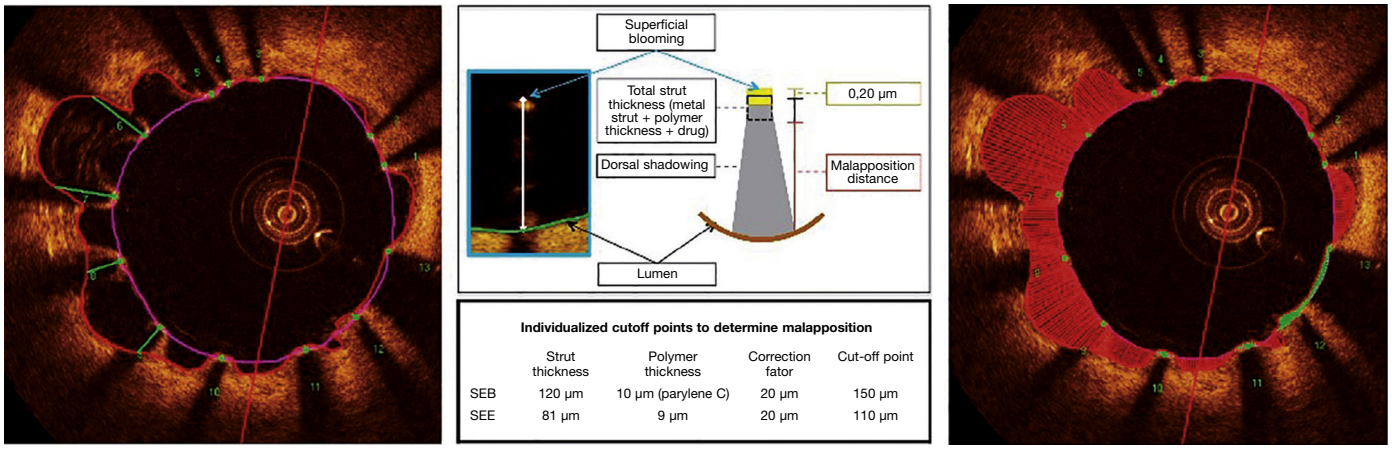

Figure 3. Malapposition. The metallic struts reflect all the light falling on their surface and produce a single hyperintense signal, which appears as intense glow (blooming), followed by intense dorsal shadowing. To determine the malapposition state, the authors used the distance from the luminal surface of the strut to the vascular lumen contour. When this distance was greater than the total strut thickness (metal strut + polymer thickness + drug), plus a 20 µm correction factor to correct for the actual location of the strut surface, it was classified as malapposed (middle panel), and the malapposition distance was computed for each individual strut (left panel). Malapposition was also quantified as the area in each frame in which it is identified along the treated segment (right panel; hatched region in red). BES: biolimus A9-eluting stent (BioMatrix™); EES: everolimus-eluting stent (XIENCE V™).

Matrix™ (n = 22) or the XIENCE V™ stent (n = 18). Of these, angiographic restudy at 6 months with IVUS and OCT was performed in 36 (90%) patients. After qualitative assessment of OCT images through core lab, a total of 26 patients were included for assessment of OCT outcomes (15 with BioMatrix™ and 11 with XIENCE V™). A flowchart detailing the inclusion of the patients in the study is shown in Figure 5.

Table 1 shows the baseline demographic characteristics, while the angiographic and procedure variables are shown in Table 2. The mean age in both groups was 58.38 ± 8.15 years, and 50% of the patients included in the study were females. Stable angina was the predominant form of clinical presentation in both groups. There was a balanced distribution among the target vessels, and B2/C lesions accounted for 42.3% of the treated lesions. The target-vessel reference diameter was 2.99 ± 0.38 mm and lesion length was 10.63 ± 4.39 mm. Predilation of the lesions was performed in only five patients from each group, while the post-dilation was performed in 90% of cases in both groups, achieving a balloon-artery ratio of 1.13 ± 0.09.

Table 1
Baseline demographic characteristics.

Variables	BioMatrix™ (n = 15)	XIENCE V™ (n = 11)	*p*-value
Age, years	56.93 ± 9.52	60.36 ± 5.64	0.30
Female gender, n (%)	10 (66.7)	3 (27.3)	0.11
Arterial hypertension, n (%)	14 (93.3)	10 (90.9)	> 0.99
Dyslipidemia, n (%)	9 (60.0)	9 (81.8)	0.40
History of smoking, n (%)	13 (86.7)	6 (54.5)	0.10
Current smoking	4 (26.7)	3 (27.3)	
Previous infarction, n (%)	7 (46.7)	4 (36.4)	0.70
Previous PCI, n (%)	1 (6.7)	0	> 0.99
Previous CABG, n (%)	0	0	> 0.99
Clinical presentation, n (%)			0.63
Silent ischemia	1 (6.7)	0	
Stable angina	12 (80.0)	10 (90.9)	
Unstable angina	2 (13.3)	1 (9.1)	

PCI: percutaneous coronary intervention; CABG: coronary artery bypass graft surgery.

OCT analysis results

From a total of 823 frames available for analysis (respecting the interval between frames of 0.6 mm), 75 frames were excluded from analysis for the following reasons: image with more than 45° of the circumference outside the field-of-view (n = 29 frames); presence of residual blood in significant amounts, preventing the visualization of the vessel intimal layer (n = 28 frames); and electronic artifacts (n = 18 frames). All 75 frames excluded were acquired using the first-generation equipment TD-OCT. In the 748 frames analyzed, 7,725 stent struts were evaluated individually. Table 3 shows the OCT analysis results.

There were no significant differences between the groups regarding the planar quantitative morphometric analysis in cross-sectional level, as well as detailed analysis at strut level. Regarding the efficacy outcomes, both stent types showed marked antiproliferative potency, as shown by the small areas (0.56 ± 0.28 mm^2 vs. 0.68 ± 0.43 mm^2; $p = 0.41$) and thickness (90.00 ± 32.75 µm vs. 96.40 ± 35.01 µm; $p = 0.64$) of neointimal hyperplasia, which resulted in a small

Table 2
Angiographic and procedural characteristics.

Variables	BioMatrix™ (n = 15)	XIENCE V™ (n = 11)	*p*-value
Target vessel, n (%)			0.44
LAD	4 (26.7)	3 (27.3)	
LCx	5 (33.3)	6 (54.5)	
RCA	6 (40.0)	2 (18.2)	
Moderate/severe calcification, n (%)	3 (20.0)	4 (36.4)	0.41
Lesion classification, n (%)			0.25
A/B1	9 (60.0)	6 (54.5)	
B2/C	6 (40.0)	5 (45.5)	
Reference vessel diameter, mm	3.05 ± 0.35	2.90 ± 0.40	0.32
Lesion length, mm	10.90 ± 3.66	10.24 ± 5.38	0.71
Minimal luminal diameter, mm	0.91 ± 0.47	1.01 ± 0.36	0.58
Diameter stenosis, %	69.86 ± 13.71	66.71 ± 11.65	0.55
Pre-dilation, n (%)	5 (33.3)	5 (45.5)	0.69
Nominal stent diameter, mm	3.17 ± 0.24	3.14 ± 0.32	0.79
Nominal stent length, mm	20.80 ± 4.59	18.55 ± 5.68	0.27
Post-dilation, n (%)	14 (93.3)	10 (90.9)	> 0.99
Balloon-artery ratio	1.11 ± 0.05	1.15 ± 0.11	0.35

LAD: left anterior descending artery; LCx: left circumflex artery; RCA: right coronary artery.

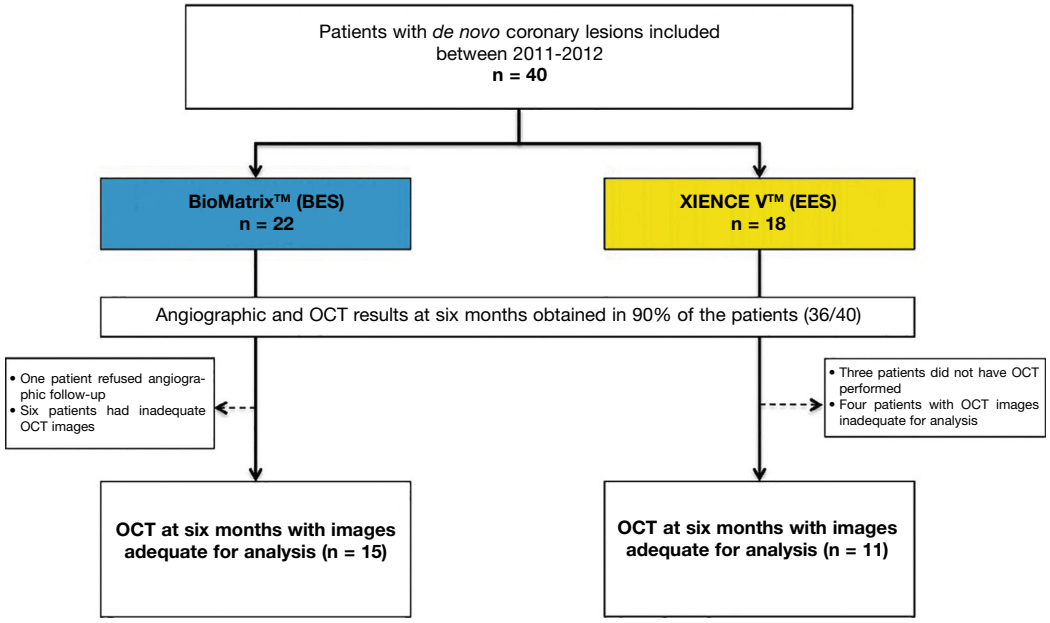

Figure 5. Study flowchart. Inclusion of patients in the study, identification of group to which they were allocated, and number of patients undergoing evaluation with optical coherence tomography (OCT). BES: A9-biolimus-eluting stent (BioMatrix™); EES: everolimus-eluting stent (XIENCE V™).

Table 3
Optical coherence tomography results.

Variables	BioMatrix™ (n = 15)	XIENCE V™ (n = 11)	*p*-value
Cross-section			
Total frames analyzed	465	284	0.20
Number of frames analyzed per patient	31.00 ± 10.50	25.72 ± 9.22	0.20
Lumen			
Mean area, mm^2	7.43 ± 3.23	6.73 ± 1.64	0.52
Minimal area, mm^2	6.10 ± 5.08	2.91 ± 1.73	0.31
Mean diameter, mm^2	3.00 ± 0.66	2.89 ± 0.36	0.64
Eccentricity index	0.13 ± 0.03	0.14 ± 0.03	0.35
Volume, mm^3	159.65 ± 88.48	118.0.6 ± 47.60	0.17
Stent			
Mean area, mm^2	7.84 ± 2.99	7.30 ± 1.70	0.60
Minimal area, mm^2	6.63 ± 2.53	6.22 ± 1.45	0.64
Mean diameter, mm	3.10 ± 0.60	3.02 ± 0.10	0.72
Eccentricity index	0.09 ± 0.02	0.09 ± 0.03	0.88
Volume, mm^3	166.96 ± 82.83	128.61 ± 54.38	0.19
Intimal hyperplasia			
Area, mm^2	0.56 ± 0.28	0.68 ± 0.43	0.41
Volume, mm^3	9.97 ± 4.45	11.69 ± 11.24	0.60
Volume obstruction, %	8.44 ± 5.10	9.21 ± 6.36	0.74
Struts			
Total struts analyzed	4,478	3,247	0.94
Number of struts analyzed per patient	298.53 ± 111.83	294.54 ± 151.00	0.94
Number of struts analyzed per frame	9.71 ± 1.84	11.04 ± 2.09	0.10
Uncovered struts per patient, %	2.10 ± 3.60	2.46 ± 2.15	0.77
Frames with > 30% uncovered struts per patient, %	1.51 ± 3.37	1.66 ± 3.47	0.91
Maximum length of segments with uncovered struts, mm	1.09 ± 1.59	1.35 ± 0.93	0.64
Malapposed struts per patient, %	0.48 ± 1.48	0.44 ± 1.05	0.94
Distance of malapposition, µm	235.00 ± 247.99	230.00 ± 306.43	0.98
Frames with > 30% malapposed struts per patient, %	0.56 ± 2.19	0.48 ± 1.59	0.91
Maximum length of segments with malapposed struts, mm	0.43 ± 1.18	0.31 ± 0.67	0.75
Intimal hyperplasia thickness on covered struts, µm	90.00 ± 32.95	96.40 ± 35.01	0.64
Stents with peri-strut infiltrate, n (%)	8 (53.3%)	3 (27.3%)	0.25
Frames with peri-strut infiltrate per patient, %	15.53 ± 20.77	11.70 ± 27.51	0.68
Stents with neoatherosclerosis, n (%)	1 (6.6%)	1 (9.1%)	> 0.99
Frames with neoatherosclerosis per patient, %	0.32 ± 1.26	2.34 ± 7.78	0.32

percentage of stent obstruction in both groups (8.44% ± 5.10% vs. 9.21% ± 6.36%; $p = 0.74$). It is noteworthy that, despite the small amount of neointimal tissue formed at the end of the 6 month period, its distribution was homogenous throughout the treated segment (Fig. 6). In fact, the percentage of uncovered struts per patient (primary surrogate safety endpoint) was low and similar between the BioMatrix™ and XIENCE V™ groups (2.10% ± 3.60% vs. 2.46% ± 2.15%; $p = 0.77$). Similarly, the incidence of malapposed struts was very low and similar in both groups (0.48% ± 1.48% vs. 0.44% ± 1.05%, $p = 0.94$) as well as the distance of malapposition of each individual strut to the vessel wall (235.00 ± 247.99 µm vs. 230.00 ± 306.43 µm; $p = 0.98$). Notably, the maximum longitudinal length of segments with uncovered (1.09 ± 1.59 mm vs. 1.35 ± 0.93 mm; $p = 0.64$) or malapposed struts (0.43 ± 1.18 mm vs. 0.31 ± 0.67 mm, $p = 0.75$) was small and similar between the groups. Figure 7 shows examples of good healing profile of the two types of stents.

In the analysis on the quality of neointimal tissue formed on the stents, the finding of peri-strut infiltrate was relatively rare, occurring in 15.53% of the frames analyzed in the BioMatrix™ group and in 11.70% of the frames analyzed in the XIENCE V™ group ($p = 0.68$). Neoatherosclerosis was observed in only one stent in each group.

Clinical outcomes

There were no cases of death or infarction during the 1-year follow-up. There were two target-lesion revascularizations – one in each group. One patient from the XIENCE V™ group had stable angina and at the time of restudy at 6 months had severe in-stent restenosis, with neoatherosclerosis findings on OCT, and thus was submitted to target-lesion revascularization. Another patient – from the BioMatrix™ group – also had stable angina at the 6-month restudy, which showed severe restenosis in the distal border of the previously implanted stent and was thus submitted to a new revascularization.

Discussion

Debates about DES safety are recurrent issues, but are still relevant. The present study used OCT to assess the antiproliferative efficacy of two types of second-generation DES, using surrogate endpoints to infer their safety in the medium term. The main findings were as follows: the incidence of uncovered or malapposed struts was low and similar in both groups after 6 months; the antiproliferative efficacy was maintained in both groups, with minimal neointimal formation, evenly distributed along the treated segments, resulting in low percentage of obstruction; both DES, utilizing different technologies, promoted "healthy" optical healing aspect, with low incidence of peri-strut infiltrate.

Although the DES were successful in achieving their primary purpose of minimizing neointimal formation and reducing rates of restenosis and new revascularizations, the excess occurrence of late and very-late thrombotic events in these devices triggered a warning sign about their safety in the long-term. Although late stent thrombosis is a multifactorial phenomenon, it has been shown that the polymers used in DES to carry and control the release of antiproliferative agents locally in the vascular wall play a key role in the genesis and perpetuation of local inflammatory processes, potentially leading to the formation of late vascular remodeling and delayed healing.[12,14,16]

Aiming to minimize the deleterious effects of polymers found in first-generation DES, a series of modifications has been promoted in

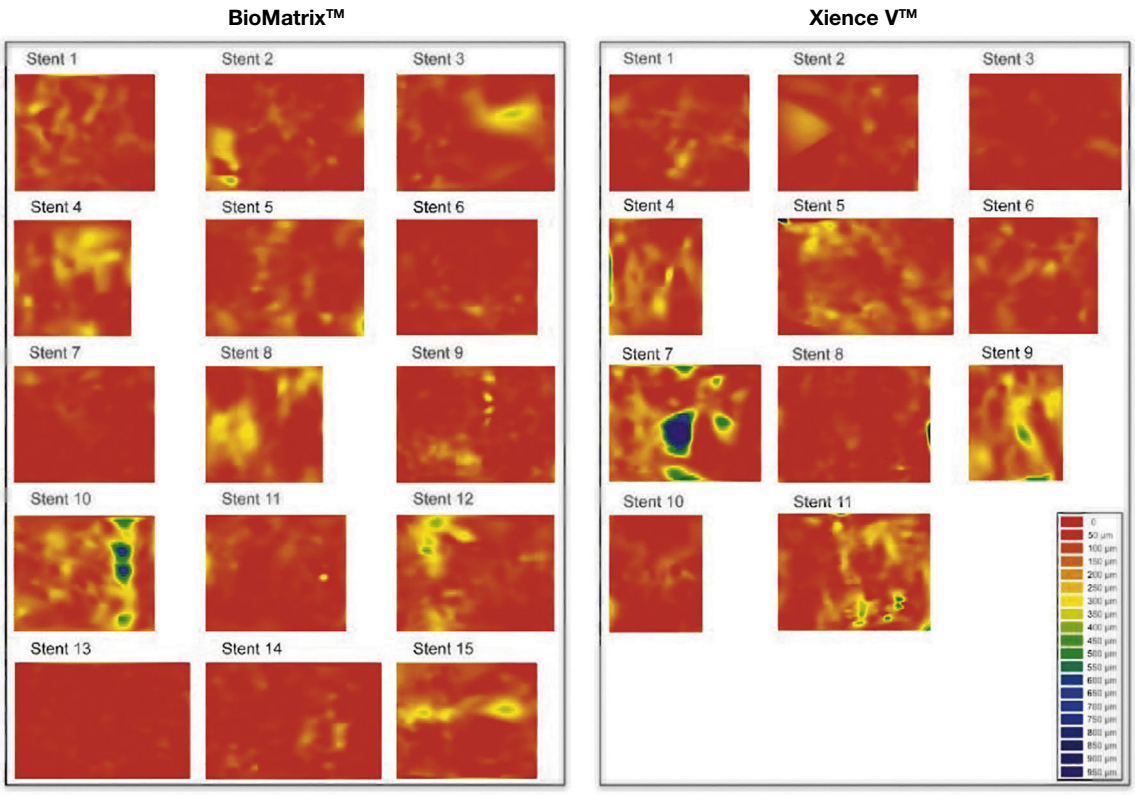

Figure 6. Dispersed neointimal topography. Neointimal tissue thickness was estimated around the 360° of circumference in each frame analyzed along the treated segment, and its distribution is shown in the circumferential and longitudinal directions of each evaluated stent. The graphs represent the stent cut longitudinally along the zero angle of the vessel circumference and arranged on a flat surface. The horizontal axis represents the stent length and the vertical axis, the 360° of its circumference. Neointimal tissue amount is represented by a color map, according to lesser (red) or greater (blue) thickness. It can be observed that both types of stents have low neointimal tissue thickness, with homogeneous distribution. Only two cases – one in each group – showed greater focal accumulation of neointimal tissue, identified by blue regions. These two patients had severe intra-segment restenosis and underwent new revascularization.

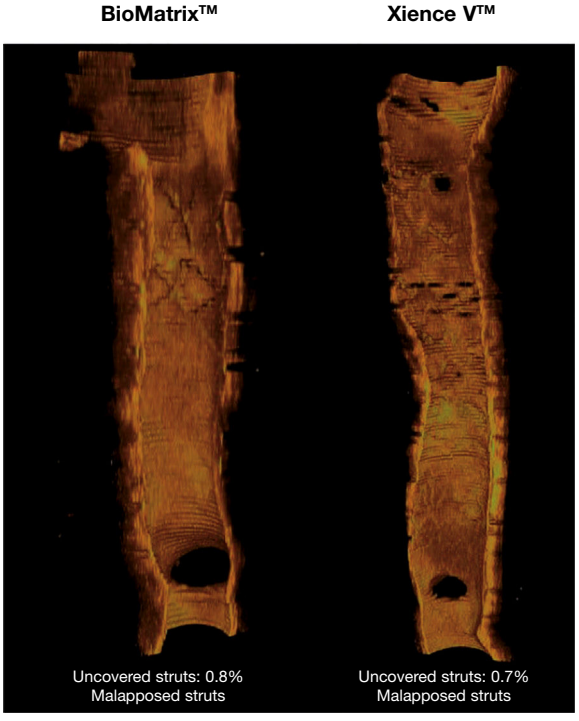

Figure 7. Healing profile of the stents. Three-dimensional reconstructions in the longitudinal direction of the BioMatrix™ and XIENCE V™ stents, illustrating the healing profile of these devices after 6 months. Note the presence of a thin neointimal tissue layer covering the entire treated segment, with a minimum percentage of uncovered struts.

the design of new generations of DES. Among these modifications, the authors highlight the use of new metal alloys, with thinner struts; more biocompatible polymers, applied only to the abluminal surface of the struts (thus reducing their thickness); bioabsorbable polymers; non-polymeric drug carrier technology; and even totally bioabsorbable stents.[17]

Incorporating some of these technological developments, the BioMatrix™ stent has a bioabsorbable PLA polymer, applied to the abluminal surface of the stent platform's stainless steel struts, which carries and releases biolimus A9. The benefits of this new second-generation DES were demonstrated in the Limus Eluted from A Durable versus ERodable Stent coating (LEADERS) trial, which conducted a randomized comparison of the clinical outcomes of the BioMatrix™ stent with the first-generation DES CYPHER™, a sirolimus-eluting stent released through a durable polymer. After 5 years, the group of patients treated with BioMatrix™ stent showed a trend to a lower incidence of major adverse cardiac events (22.3% vs. 26.1%; $p = 0.071$), in addition to a significant reduction in rates of late stent thrombosis after the first year (0.66% vs. 2.5%; $p = 0.003$).[27] The OCT sub-analysis of this study showed a better healing profile with the BioMatrix™ stent, with a lower percentage of uncovered struts when compared with the CYPHER™ stent (0.6% vs. 2.1%, $p = 0.04$) at the end of 9 months.[28]

Similarly, the second-generation DES XIENCE V™ was also compared to the CYPHER™ stent in the randomized trial Scandinavian Organization for Randomized Trials with Clinical Outcome IV (SORT OUT IV). At the end of 9 months, the occurrence of the primary endpoint (cardiac death, myocardial infarction, definitive stent thrombosis, and target-vessel revascularization) was similar between the two types of DES (4.9% vs. 5.2%, p for non-inferiority = 0.01).[29] These

results were maintained until the end of the 2-year follow-up (8.3% vs. 8.7%; $p = 0.66$).[30] Importantly, the XIENCE V™ stent, which similarly to the CYPHER™ stent has durable polymer, but is thinner and more biocompatible, showed a strong trend toward a lower incidence of definitive stent thrombosis at 9 months (0.1% vs. 0.7%, $p = 0.05$),[29] which was significantly confirmed at the end of 2 years (0.2% vs. 0.9%; $p = 0.02$).[30]

After verifying the non-inferiority of the second-generation DES when compared to first-generation DES regarding their antiproliferative efficiency, but featuring a better safety profile,[31] it was not long before the first comparisons between second-generation DES started to appear.

The Comparison of the Everolimus Eluting with the Biolimus A9 Eluting Stent (COMPARE-II) trial compared, in a randomized manner (2:1), 2,707 patients for treatment with Nobori™ stents (n = 1,795; Terumo, Tokyo, Japan), which, similarly to BioMatrix™ stents, release biolimus A9 through a bioabsorbable polymer, or with everolimus-eluting stents through a durable fluoropolymer (XIENCE V™ or XIENCE PRIME™; n = 912). The occurrence of the primary endpoint (cardiac death, nonfatal myocardial infarction, and target-vessel revascularization guided by ischemia) at 12 months was similar in both groups (Nobori™: 5.2% vs. XIENCE V™: 4.8%; *p* for non-inferiority < 0.0001).[32] These results are echoed in the OCT evaluation of these two stent types performed by Tada et al., who found no significant differences regarding the percentage of strut coverage between the second-generation DES Nobori™ and XIENCE V™ (OR = 1.54; 95%CI 0.63-3.79; $p = 0.34$) after 6 to 8 months.

The present study confirmed the excellent healing profile of XIENCE V™ and BioMatrix™ stents, which demonstrated potent suppression in neointimal formation intensity without affecting the healing profile, as demonstrated by the low percentage of uncovered struts. However, a longer follow-up is required to assess the potential benefits of DES with durable polymers.

Evolution in the evaluation of new drug-eluting stents and the contribution of optical coherence tomography

The evolution of invasive imaging methods has coincided with technological advances in interventional cardiology. Throughout history, intravascular imaging methods have contributed to the understanding of the mechanism of action in different devices, helping to understand possible failure mechanisms and providing for technological advancement.

Historically, the late performance of a coronary stent was evaluated for its efficacy in suppressing neointimal tissue formation – often evaluated by late luminal loss at angiography and quantification, by IVUS, of neointimal hyperplasia volume and the degree to which this tissue obstructs stent area (the percentage of obstruction). However, the demonstration, through histopathological studies, that the absence or delay in stent strut healing was among the most powerful pathological predictors for the occurrence of late thrombosis in these devices[13,16] induced reflection about the *in vivo* evaluation of coronary stents. The focus was no longer only the assessment of the antiproliferative stent potency, but also the quantitation of morphometric markers indicative of safety. Thus, the percentage of coverage and apposition of coronary stent struts started to be used as a primary endpoint in a number of randomized studies designed to evaluate the performance of different DES over variable periods.[33]

While BMS usually develop a circumferential coverage of neointimal tissue with a mean thickness of 500 μm (late luminal loss of approximately 1 mm) – easily identified and quantified by angiography and IVUS – DES show a delayed and even null hyperplastic response that is so intense that their struts are often covered by a thin tissue layer, whose thickness is well below the detection limits of angiography and IVUS. Due to its high axial resolution (ten times greater than that provided by IVUS), OCT was demonstrated to be more sensitive and accurate than the IVUS to identify coverage and malapposition of stent struts,[34-36] showing good correlation with histological assessment[18,36-38] and high reproducibility.[18,38] Therefore, OCT allows for the assessment of complex stent-vessel interaction *in vivo* with an unprecedented level of detail, and thus became the standard imaging modality for vascular response assessment after stent implantation in a number of randomized studies.[33] In the present study, the mean thickness of the neointimal tissue formed at the end of 6 months was less than 100 μm and was below the detection limits of the IVUS.

In addition to the abovementioned accurate quantitative assessment, OCT also allows for the identification of the quality of the neointimal tissue formed. At the beginning of DES evaluations with OCT, it was not rare to observe areas of low optical signal intensity in the neointimal tissue around the stent struts. These findings, known as peri-strut infiltrates (or PLIA, peri-strut low intensity areas) showed correspondence, at the histological findings, with hypocellular regions and the presence of fibrinoid material and proteoglycans, surrounded by a polymorphic healing response with macrophages and lymphocytes.[25] A pathological study carried out by van Beusekom et al. showed the presence of acellular areas after first-generation DES implantation, which did not exist with BMS.[39] These findings were confirmed *in vivo* in the assessment of 36 stents, in which peri-strut infiltrates were more frequently identified in DES (65%) than in BMS (19%; $p < 0.001$), suggesting a local adverse reaction to the drug and/or polymer.[25] Neoatherosclerosis is a phenomenon that refers to the formation of new atherosclerotic plaque inside an already-formed neointima. The degeneration of a normal neointima, with the development of vulnerable plaques and their eventual rupture, has been recently identified as a cause of late stent failure – again, more frequently identified after DES implantation.[40] In the present study, the incidence of peri-strut infiltrate was lower than that observed after first-generation DES implantation, suggesting, in theory, a more benign vascular response after second-generation DES implantation. The actual clinical impact of these findings remains to be investigated in larger studies with a longer follow-up period. In the present population, the incidence of neoatherosclerosis was low, represented by one case in each group. However, it was associated with more exacerbated neointimal proliferation in one case, which required revascularization.

Limitations

Some limitations of the present study are worth mentioning. First, although the included population provided enough data (749 frames and 7,725 struts analyzed) for evaluation of surrogate endpoints of efficacy and safety by OCT, the number of patients included is insufficient to assess the clinical impact of the findings on OCT. Second, non-performance of the OCT after the index procedure prevents a temporal classification of observed malappositions; it is not possible to determine whether a malapposition identified at 6 months is only the residual effect of an acute malapposition, or whether it was acquired later. However, the low incidence and magnitude of the malappositions, observed in the context of favorable stent healing, suggest that the few malappositions observed in this study do not represent unfavorable local vascular reactions. Third, the 6-month evaluation period appears to be a short time to detect potential differences between the two stents evaluated. It is unknown whether the favorable vascular responses observed in the present study will remain in the long-term follow-up. Fourth, the population included in this analysis consisted predominantly of stable patients without diabetes and with relatively short lesions in larger vessels. This selection was aimed to minimize the inclusion of patients with more advanced disease, which could impact the assessment of endothelial function – one of the primary BIOACTIVE

study endpoints. Thus, extrapolation of the results shown here to more complex populations should be performed with caution.

Conclusions

The second-generation drug-eluting stents BioMatrix™ and XIENCE V™ showed favorable vascular response after 6 months. These two types of drug-eluting stents demonstrated excellent efficacy profiles, with effective suppression of neointimal formation and low percentage of in-stent obstruction, without causing delay in strut coverage, as shown by the low and comparable rates of non-covered and malapposed struts. In addition, the healing quality was also favorable, with reduced rates of peri-strut infiltrate and neoatherosclerosis.

Funding sources

None declared.

Conflicts of interest

The authors declare no conflicts of interest.

References

1. Sousa JE, Costa MA, Abizaid A, Abizaid AS, Feres F, Pinto IM, et al. Lack of neointimal proliferation after implantation of sirolimus-coated stents in human coronary arteries: a quantitative coronary angiography and three-dimensional intravascular ultrasound study. Circulation. 2001;103(2):192-5.
2. Sousa JE, Costa MA, Abizaid AC, Rensing BJ, Abizaid AS, Tanajura LF, et al. Sustained suppression of neointimal proliferation by sirolimus-eluting stents: one-year angiographic and intravascular ultrasound follow-up. Circulation. 2001;104(17):2007-11.
3. Morice MC, Serruys PW, Sousa JE, Fajadet J, Ban Hayashi E, Perin M, et al.; RAVEL Study Group. Randomized Study with the Sirolimus-Coated Bx Velocity Balloon-Expandable Stent in the Treatment of Patients with de Novo Native Coronary Artery Lesions. A randomized comparison of a sirolimus-eluting stent with a standard stent for coronary revascularization. N Engl J Med. 2002;346(23):1773-80.
4. Stone GW, Ellis SG, Cox DA, Hermiller J, O'Shaughnessy C, Mann JT, et al.; TAXUS-IV Investigators. One-year clinical results with the slow-release, polymer-based, paclitaxel-eluting TAXUS stent: the TAXUS-IV trial. Circulation. 2004;109(16):1942-7.
5. Sousa JE, Costa MA, Abizaid A, Sousa AG, Feres F, Mattos LA, et al. Sirolimus-eluting stent for the treatment of in-stent restenosis: a quantitative coronary angiography and three-dimensional intravascular ultrasound study. Circulation. 2003;107(1):24-7.
6. Stone GW, Ellis SG, Cannon L, Mann JT, Greenberg JD, Spriggs D, et al. Comparison of a polymer-based paclitaxel-eluting stent with a bare metal stent in patients with complex coronary artery disease: a randomized controlled trial. JAMA. 2005;294(10):1215-23.
7. Baumgart D, Klauss V, Baer F, Hartmann F, Drexler H, Motz W, et al.; SCORPIUS Study Investigators. One-year results of the SCORPIUS study: a German multicenter investigation on the effectiveness of sirolimus-eluting stents in diabetic patients. J Am Coll Cardiol. 2007;50(17):1627-34.
8. Daemen J, van Twisk PH, Kukreja N, van Domburg RT, Boersma E, de Jaegere P, et al. The relative safety and efficacy of bare-metal and drug-eluting stents in low and high-risk patient subsets. An epidemiological analysis of three sequential cohorts of consecutive all comers (n = 6129). EuroIntervention. 2009;4(4):464-74.
9. Camenzind E, Steg PG, Wijns W. Stent thrombosis late after implantation of first-generation drug-eluting stents: a cause for concern. Circulation. 2007;115(11):1440-55; discussão 1455.
10. Daemen J, Wenaweser P, Tsuchida K, Abrecht L, Vaina S, Morger C, et al. Early and late coronary stent thrombosis of sirolimus-eluting and paclitaxel-eluting stents in routine clinical practice: data from a large two-institutional cohort study. Lancet. 2007;369(9562):667-78.
11. Lagerqvist B, James SK, Stenestrand U, Lindbäck J, Nilsson T, Wallentin L; SCAAR Study Group. Long-term outcomes with drug-eluting stents versus bare-metal stents in Sweden. N Engl J Med. 2007;356(10):1009-19.
12. Virmani R, Guagliumi G, Farb A, Musumeci G, Grieco N, Motta T, et al. Localized hypersensitivity and late coronary thrombosis secondary to a sirolimus-eluting stent: should we be cautious? Circulation. 2004;109(6):701-5.
13. Joner M, Finn AV, Farb A, Mont EK, Kolodgie FD, Ladich E, et al. Pathology of drug-eluting stents in humans: delayed healing and late thrombotic risk. J Am Coll Cardiol. 2006;48(1):193-202.
14. Nebeker JR, Virmani R, Bennett CL, Hoffman JM, Samore MH, Alvarez J, et al. Hypersensitivity cases associated with drug-eluting coronary stents: a review of available cases from the Research on Adverse Drug Events and Reports (RADAR) project. J Am Coll Cardiol. 2006;47(1):175-81.
15. Kotani J, Awata M, Nanto S, Uematsu M, Oshima F, Minamiguchi H, et al. Incomplete neointimal coverage of sirolimus-eluting stents: angioscopic findings. J Am Coll Cardiol. 2006;47(10):2108-11.
16. Finn AV, Joner M, Nakazawa G, Kolodgie F, Newell J, John MC, et al. Pathological correlates of late drug-eluting stent thrombosis: strut coverage as a marker of endothelialization. Circulation. 2007;115(18):2435-41.
17. Stefanini GG, Taniwaki M, Windecker S. Coronary stents: novel developments. Heart 2014;100(13):1051-61.
18. Murata A, Wallace-Bradley D, Tellez A, Alviar C, Aboodi M, Sheehy A, et al. Accuracy of optical coherence tomography in the evaluation of neointimal coverage after stent implantation. JACC Cardiovasc Imaging. 2010;3(1):76-84.
19. Templin C, Meyer M, Muller MF, Djonov V, Hlushchuk R, Dimova I, et al. Coronary optical frequency domain imaging (OFDI) for in vivo evaluation of stent healing: comparison with light and electron microscopy. Eur Heart J. 2010;31(14):1792-801.
20. Levine GN, Bates ER, Blankenship JC, Bailey SR, Bittl JA, Cercek B, et al.; American College of Cardiology Foundation; American Heart Association Task Force on Practice Guidelines; Society for Cardiovascular Angiography and Interventions. 2011 ACCF/AHA/SCAI Guideline for Percutaneous Coronary Intervention. A report of the American College of Cardiology Foundation/American Heart Association Task Force on Practice Guidelines and the Society for Cardiovascular Angiography and Interventions. J Am Coll Cardiol. 2011;58(24):e44-122.
21. Authors/Task Force members; Windecker S, Kolh P, Alfonso F, Collet JP, Cremer J, et al. 2014 ESC/EACTS Guidelines on myocardial revascularization: The Task Force on Myocardial Revascularization of the European Society of Cardiology (ESC) and the European Association for Cardio-Thoracic Surgery (EACTS) Developed with the special contribution of the European Association of Percutaneous Cardiovascular Interventions (EAPCI). Eur Heart J. 2014;35(37):2541-619.
22. Tanigawa J, Barlis P, Di Mario C. Intravascular optical coherence tomography: optimisation of image acquisition and quantitative assessment of stent strut apposition. EuroIntervention. 2007;3(1):128-36.
23. Chamié D, Bezerra HG, Attizzani GF, Yamamoto H, Kanaya T, Stefano GT, et al. Incidence, predictors, morphological characteristics, and clinical outcomes of stent edge dissections detected by optical coherence tomography. JACC Cardiovasc Interv. 2013;6(8):800-13.
24. Okamura T, Gonzalo N, Gutiérrez-Chico JL, Serruys PW, Bruining N, de Winter S, et al. Reproducibility of coronary Fourier domain optical coherence tomography: quantitative analysis of in vivo stented coronary arteries using three different software packages. EuroIntervention. 2010;6(3):371-9.
25. Teramoto T, Ikeno F, Otake H, Lyons JK, van Beusekom HM, Fearon WF, et al. Intriguing peri-strut low-intensity area detected by optical coherence tomography after coronary stent deployment. Circ J. 2010;74(6):1257-9.
26. Kang SJ, Mintz GS, Akasaka T, Park DW, Lee JY, Kim WJ, et al. Optical coherence tomographic analysis of in-stent neoatherosclerosis after drug-eluting stent implantation. Circulation. 2011;123(25):2954-63.
27. Serruys PW, Farooq V, Kalesan B, de Vries T, Buszman P, Linke A, et al. Improved safety and reduction in stent thrombosis associated with biodegradable polymer-based biolimus-eluting stents versus durable polymer-based sirolimus-eluting stents in patients with coronary artery disease: final 5-year report of the LEADERS (Limus Eluted From A Durable Versus ERodable Stent Coating) randomized, noninferiority trial. JACC Cardiovasc Interv. 2013;6(8):777-89.
28. Barlis P, Regar E, Serruys PW, Dimopoulos K, van der Giessen WJ, van Geuns RJ, et al. An optical coherence tomography study of a biodegradable vs. durable polymer-coated limus-eluting stent: a LEADERS trial sub-study. Eur Heart J. 2010;31(2):165-76.
29. Jensen LO, Thayssen P, Hansen HS, Christiansen EH, Tilsted HH, Krusell LR, et al.; Scandinavian Organization for Randomized Trials With Clinical Outcome IV (SORT OUT IV) Investigators. Randomized comparison of everolimus-eluting and sirolimus-eluting stents in patients treated with percutaneous coronary intervention: the Scandinavian Organization for Randomized Trials with Clinical Outcome IV (SORT OUT IV). Circulation. 2012;125(10):1246-55.
30. Jensen LO, Thayssen P, Christiansen EH, Tilsted HH, Maeng M, Hansen KN, et al.; SORT OUT IV Investigators. 2-year patient-related versus stent-related outcomes: the SORT OUT IV (Scandinavian Organization for Randomized Trials With Clinical Outcome IV) Trial. J Am Coll Cardiol. 2012;60(13):1140-7.
31. Bangalore S, Kumar S, Fusaro M, Amoroso N, Attubato MJ, Feit F, et al. Short- and long-term outcomes with drug-eluting and bare-metal coronary stents: a mixed-treatment comparison analysis of 117 762 patient-years of follow-up from randomized trials. Circulation. 2012;125(23):2873-91.
32. Smits PC, Hofma S, Togni M, Amoroso N, Attubato MJ, Feit F, et al. Abluminal biodegradable polymer biolimus-eluting stent versus durable polymer everolimus-eluting stent (COMPARE II): a randomised, controlled, non-inferiority trial. Lancet. 2013;381:651-60.
33. Tahara S, Chamie D, Baibars M, Alraies C, Costa M. Optical coherence tomography endpoints in stent clinical investigations: strut coverage. Int J Cardiovasc Imaging. 2011;27(2):271-87.
34. Bouma BE, Tearney GJ, Yabushita H, Shishkov M, Kauffman CR, DeJoseph Gauthier D, et al. Evaluation of intracoronary stenting by intravascular optical coherence tomography. Heart. 2003;89(3):317-20.

35. Matsumoto D, Shite J, Shinke T, Otake H, Tanino Y, Ogasawara D, et al. Neointimal coverage of sirolimus-eluting stents at 6-month follow-up: evaluated by optical coherence tomography. Eur Heart J. 2007;28(8):961-7.
36. Suzuki Y, Ikeno F, Koizumi T, Tio F, Yeung AC, Yock PG, et al. In vivo comparison between optical coherence tomography and intravascular ultrasound for detecting small degrees of in-stent neointima after stent implantation. JACC Cardiovasc Interv. 2008;1(2):168-73.
37. Prati F, Zimarino M, Stabile E, Pizzicannella G, Fouad T, Rabozzi R, et al. Does optical coherence tomography identify arterial healing after stenting? An in vivo comparison with histology, in a rabbit carotid model. Heart. 2008;94(2):217-21.
38. Capodanno D, Prati F, Pawlowsky T, Cera M, La Manna A, Albertucci M, et al. Comparison of optical coherence tomography and intravascular ultrasound for the assessment of in-stent tissue coverage after stent implantation. EuroIntervention. 2009;5(5):538-43.
39. van Beusekom HM, Saia F, Zindler JD, Lemos PA, Swager-Ten Hoor SL, van Leeuwen MA, et al. Drug-eluting stents show delayed healing: paclitaxel more pronounced than sirolimus. Eur Heart J. 2007;28(8):974-9.
40. Nakazawa G, Otsuka F, Nakano M, Vorpahl M, Yazdani SK, Ladich E, et al. The pathology of neoatherosclerosis in human coronary implants bare-metal and drug-eluting stents. J Am Coll Cardiol. 2011;57(11):1314-22.